

# Balanced truncation with conformal maps

Alessandro Borghi<sup>†</sup>   Tobias Breiten<sup>†</sup>   Serkan Gugercin<sup>‡</sup>

<sup>†</sup>*Technical University of Berlin, Mathematics Department, Straße des 17. Juni 136, 10623 Berlin, Germany.*

Email: [borghi@tu-berlin.de](mailto:borghi@tu-berlin.de), ORCID: 0000-0002-5333-3074

Email: [tobias.breiten@tu-berlin.de](mailto:tobias.breiten@tu-berlin.de), ORCID: 0000-0002-9815-4897

<sup>‡</sup>*Department of Mathematics and Division of Computational Modeling and Data Analytics, Academy of Data Science, Virginia Tech, Blacksburg, VA 24061, USA.*

Email: [gugercin@vt.edu](mailto:gugercin@vt.edu), ORCID: 0000-0003-4564-5999

**Abstract:** We consider the problem of constructing reduced models for large scale systems with poles in general domains in the complex plane (as opposed to, e.g., the open left-half plane or the open unit disk). Our goal is to design a model reduction scheme, building upon theoretically established methodologies, yet encompassing this new class of models. To this aim, we develop a balanced truncation framework through conformal maps to handle poles in general domains. The major difference from classical balanced truncation resides in the formulation of the Gramians. We show that these new Gramians can still be computed by solving modified Lyapunov equations for specific conformal maps. A numerical algorithm to perform balanced truncation with conformal maps is developed and is tested on three numerical examples, namely a heat model, the Schrödinger equation, and the undamped linear wave equation, the latter two having spectra on the imaginary axis.

**Keywords:** model order reduction, balanced truncation, conformal mapping

**Mathematics subject classification:** 34C20, 41A20, 93A15, 93C05

## 1 Introduction

We consider large-scale linear time invariant (LTI) systems of the form

$$\begin{cases} \dot{\mathbf{x}}(t) = \mathbf{A}\mathbf{x}(t) + \mathbf{B}\mathbf{u}(t), \\ \mathbf{y}(t) = \mathbf{C}\mathbf{x}(t), \quad \mathbf{x}(0) = 0, \end{cases} \quad (1)$$

with  $\mathbf{A} \in \mathbb{C}^{n \times n}$ ,  $\mathbf{B} \in \mathbb{C}^{n \times m}$ , and  $\mathbf{C} \in \mathbb{C}^{q \times n}$ . In (1),  $\mathbf{x}(t) \in \mathbb{C}^n$ ,  $\mathbf{u}(t) \in \mathbb{C}^m$ , and  $\mathbf{y}(t) \in \mathbb{C}^q$  denote, respectively, the states, inputs, and outputs of the LTI system. Throughout the paper we mainly consider the frequency domain description of (1) given by the transfer function

$$\mathbf{G}(\cdot) = \mathbf{C}(\cdot\mathbf{I} - \mathbf{A})^{-1}\mathbf{B}. \quad (2)$$

The system described by (1) and (2) is referred to as the full order model (FOM). In the case of a large scale system the computational effort to solve (1) for different input signals can often be prohibitive. The aim of model order reduction

is to compute a reduced order model (ROM) that resembles the input output behaviour of (1) while drastically lowering the state dimension. More specifically, the objective is to determine a surrogate model of (1) with the same structure, i.e.,

$$\begin{cases} \dot{\mathbf{x}}_r(t) = \mathbf{A}_r\mathbf{x}_r(t) + \mathbf{B}_r\mathbf{u}(t), \\ \mathbf{y}_r(t) = \mathbf{C}_r\mathbf{x}_r(t), \quad \mathbf{x}_r(0) = 0, \end{cases} \quad (3)$$

and transfer function

$$\mathbf{G}_r(\cdot) = \mathbf{C}_r(\cdot\mathbf{I} - \mathbf{A}_r)^{-1}\mathbf{B}_r, \quad (4)$$

where  $\mathbf{A}_r \in \mathbb{C}^{r \times r}$ ,  $\mathbf{B}_r \in \mathbb{C}^{r \times m}$ , and  $\mathbf{C}_r \in \mathbb{C}^{q \times r}$ , such that the output behaviour  $\mathbf{y}_r$  well approximates  $\mathbf{y}$  for a set of inputs  $\mathbf{u}$ . In particular, for the model to be computationally efficient, we impose  $r \ll n$ . As a metric of disparity between the two models  $\mathbf{G}$  and  $\mathbf{G}_r$ , generally the  $\mathcal{H}_\infty$  or the  $\mathcal{H}_2$  norms are used (see, e.g., [1, Section 5.1.3]).

Many model order reduction techniques have been developed to approximate the systems of the form (1). We re-

fer the reader to [1–5, 17, 19] and the extensive references therein for a detailed overview of different techniques. The framework developed in this article is closely related to balanced truncation (BT) [15, 16], one of the gold standards in system theoretic approaches to model reduction, and its extension to structured differential equations [7, 18]. In this paper, we focus on the classical Lyapunov balancing; for details on the other variants of BT, we refer the reader to the survey articles [8, 12]. Furthermore, here we focus on the projection-based formulation of BT. For a data-driven formulation of BT using only transfer function evaluations, see [11].

In this paper, we assume that the poles of  $\mathbf{G}$ , i.e., the eigenvalues of  $\mathbf{A}$ , lie in  $\mathbb{A} \subset \mathbb{C}$ , a non-empty connected open set (which is not necessarily the open left-half plane as usually assumed). We then adopt the conformal mapping framework introduced in [6] to extend BT to LTI systems with poles in general domains  $\mathbb{A} \subset \mathbb{C}$ . More specifically, the main contributions are the following:

1. Via conformal mappings, we develop the Gramians of an LTI system with poles in general domains and, consequently, we extend the balanced truncation algorithm to this class of systems.
2. We prove that, for some choice of conformal mappings, the Gramians are the solutions of modified Lyapunov equations.
3. We prove that the resulting reduced model preserves stability when specific conformal maps are adopted. In addition, we provide an a-posteriori bound on an appropriately modified  $\mathcal{H}_2$  like norm.
4. We develop an algorithmic framework and show the effectiveness of the proposed method on a diverse set of examples with poles in different domains.

The structure of the paper is as follows. In Section 2 we review some basic facts on conformal maps and balanced truncation. Section 3 introduces our main result, a conformal mapping framework for BT, and the corresponding algorithm. In Section 4 we discuss some theoretical results on BT with conformal maps. Specifically, we prove stability preservation of the reduced model when specific conformal maps are used, and develop a bound on the  $\mathcal{H}_2$  error norm. Three numerical experiments with the proposed algorithm are provided in Section 5. Here, we use partial differential equations with spectra on the left-half complex plane and on the imaginary axis.

## 1.1 Notation

Throughout the paper we indicate with  $\|\cdot\|_F$  the Frobenius norm and  $\|\cdot\|_2$  the spectral norm. The absolute value of a

complex number  $z$  is denoted by  $|z| = \sqrt{zz^*}$ . The symbol  $i$  indicates the imaginary unit. The symbol  $(\cdot)^*$  indicates the complex conjugation of a scalar or the conjugate transpose of a matrix. If  $\mathbb{A}$  is an open subset of the complex plane,  $\partial\mathbb{A}$  denotes its boundary,  $\bar{\mathbb{A}} = \{\mathbb{A} \cup \partial\mathbb{A}\}$  its closure,  $\mathbb{A}^c$  its complement, and  $\bar{\mathbb{A}}^c = \{\mathbb{C} \setminus \bar{\mathbb{A}}\}$  its exterior. The symbols  $\mathbb{C}$ ,  $\mathbb{C}_-$ , and  $\mathbb{C}_+$  stand for the complex plane, the open left-half complex plane, and the open right-half complex plane, respectively. In addition,  $\mathbb{R}$  and  $i\mathbb{R}$  indicate the real numbers and the imaginary numbers, respectively. For a single-variable complex-valued differentiable bijective function  $f$  we indicate its complex derivative by  $f'$  and its inverse by  $f^{-1}$ . In addition, for a complex-valued function  $g$ , we indicate the composition of  $f$  and  $g$  as  $f \circ g$  or  $f(g(\cdot))$ . For the numerical examples, spatially localized controls on intervals  $[a, b]$  are addressed with the indicator function  $\chi_{[a,b]}$ .

## 2 Preliminaries

### 2.1 A conformal mapping framework

As stated in Section 1, this paper considers LTI systems with poles in general domains  $\mathbb{A}$  that are not necessarily the unit disk nor the left-half plane. For the FOM with transfer function (2), to simplify the presentation, we assume that  $\mathbf{A}$  has the eigendecomposition  $\mathbf{A} = \mathbf{V}\mathbf{\Lambda}\mathbf{V}^{-1}$ ,  $\mathbf{\Lambda} = \text{diag}(\lambda_1, \dots, \lambda_n)$ , with simple eigenvalues. As we discuss in Remark 1 the analysis can be extended to the general case via Schur decomposition. For  $\mathbb{A} \subset \mathbb{C}$  being a non-empty connected open set, we then have that  $\lambda_j \in \mathbb{A}$ , for  $j = 1, \dots, n$ . To adapt balanced truncation to this type of systems, we develop a new framework that relies on conformal maps. For this reason, we recall the conformal mapping theorem below.

**Theorem 1** ([20], Theorem 6.1.2). *Suppose  $\mathbb{X}, \mathbb{Y} \subset \mathbb{C}$  are open sets and let  $\psi: \mathbb{X} \rightarrow \mathbb{Y}$  be Fréchet differentiable as a function of two real variables. The mapping  $\psi$  is conformal in  $\mathbb{X}$  if and only if it is analytic in  $\mathbb{X}$  and  $\psi'(z_0) \neq 0$  for every  $z_0 \in \mathbb{X}$ .*

Throughout the paper, we make the following assumptions

**Assumption 1.** *We assume that*

(2.1)  $\psi: \mathbb{X} \rightarrow \mathbb{A}$  is a bijective conformal map where  $\mathbb{X} \subseteq \mathbb{C}_-$  such that its boundary  $\partial\mathbb{X}$  includes the imaginary axis  $i\mathbb{R}$ .

(2.2)  $\psi: \tilde{\mathbb{X}} \rightarrow \bar{\mathbb{A}}^c$  is also conformal with  $\tilde{\mathbb{X}} \subseteq \mathbb{C} \setminus \{\mathbb{X} \cup i\mathbb{R}\}$ .

(2.3) Let  $\partial\mathbb{A}^+$  the boundary of  $\mathbb{A}$  such that its interior includes the eigenvalues of  $\mathbf{A}$ , we then consider  $\psi \circ i: \mathbb{R} \rightarrow \partial\mathbb{A}^+$  to be continuously differentiable and  $\psi'(z) \neq 0$  for every  $z \in \mathbb{R}$ .

A simplified graphical depiction of [Assumption 1](#) is given in [Fig. 1](#) (a more involved example is given in [Fig. 4](#)). Note that, by the inverse mapping theorem, [Assumption 1.3](#) guarantees bijectivity of  $\psi$  on the imaginary axis. Some of the main results in this paper, specifically [Theorem 2](#) and [Theorem 3](#), use a Möbius transformation  $m$  as conformal map satisfying [Assumption 1](#). The Möbius transformation  $m$  and its inverse are given by

$$m(\cdot) = \frac{\alpha \cdot + \beta}{\gamma \cdot + \delta}, \quad m^{-1}(\cdot) = \frac{\beta - \delta \cdot}{\gamma \cdot - \alpha}, \quad (5)$$

with  $\alpha, \beta, \gamma, \delta \in \mathbb{C}$  and  $\alpha\delta - \beta\gamma \neq 0$ .

We refer the reader to [\[20, Section 6.3\]](#) for more details. In addition, we also apply the Möbius transformation to matrices. Consider the matrix  $\mathbf{A}$ , we then have the following definitions:

$$m(\mathbf{A}) = (\alpha \mathbf{A} + \beta \mathbf{I})(\gamma \mathbf{A} + \delta)^{-1}, \quad (6)$$

$$m^{-1}(\mathbf{A}) = (\beta \mathbf{I} - \delta \mathbf{A})(\gamma \mathbf{A} - \alpha \mathbf{I})^{-1},$$

with the parameters  $\alpha, \beta, \gamma, \delta$  being as in [\(5\)](#). In this manuscript, the application of a scalar function  $m$  to a matrix  $\mathbf{A}$  follows the definition given in [\[13\]](#). More in detail, for the eigendecomposition of  $\mathbf{A}$ , we define

$$m(\mathbf{A}) := \mathbf{V}m(\boldsymbol{\Lambda})\mathbf{V}^{-1} = \mathbf{V} \begin{bmatrix} m(\lambda_1) & & \\ & \ddots & \\ & & m(\lambda_n) \end{bmatrix} \mathbf{V}^{-1}.$$

A similar definition applies for  $m^{-1}$ .

In the next section, we introduce a space of square integrable functions with poles in general domains.

## 2.2 The $\mathcal{H}_2(\bar{\mathbb{A}}^c)$ space

In model order reduction,  $\mathcal{H}_2$  denotes a particular Hardy space. More precisely, it denotes the Hilbert space consisting of all functions  $\mathbf{F}$  and  $\mathbf{H}$ , respectively, analytic in  $\mathbb{C}_+$  satisfying

$$\sup_{x>0} \int_{-\infty}^{\infty} \|\mathbf{F}(x+i\omega)\|_{\mathbb{F}}^2 d\omega < \infty$$

with the inner product

$$\langle \mathbf{F}, \mathbf{H} \rangle_{\mathcal{H}_2} := \frac{1}{2\pi} \int_{-\infty}^{\infty} \text{trace} \{ \mathbf{F}(i\omega) \mathbf{H}(i\omega)^* \} d\omega,$$

and the corresponding norm

$$\|\mathbf{F}\|_{\mathcal{H}_2} := \left( \frac{1}{2\pi} \int_{-\infty}^{\infty} \|\mathbf{F}(i\omega)\|_{\mathbb{F}}^2 d\omega \right)^{\frac{1}{2}}.$$

In the cases studied in this paper,  $\mathbf{F}$  is analytic in  $\bar{\mathbb{A}}^c$ . Here,  $\bar{\mathbb{A}}^c$  does not necessarily have to be the open right half complex plane, meaning that  $\mathbf{F}$  is not necessarily in  $\mathcal{H}_2$ . Due

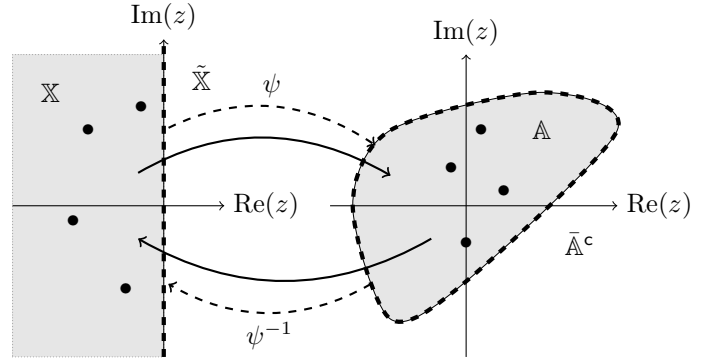


Figure 1: An illustration of a conformal map satisfying [Assumption 1](#). The arrows between the grey sets  $\mathbb{X}$  and  $\mathbb{A}$  indicate the bijectivity of  $\psi$ . The same holds for the dashed arrow lines between the dashed boundaries  $i\mathbb{R}$  and  $\partial\mathbb{A}^+$  (in this depiction  $\partial\mathbb{A}^+$  coincides with  $\partial\mathbb{A}$ ). The dots  $\bullet$  indicate the poles of the transfer function  $\mathbf{G}$ . In addition,  $\psi$  conformally maps the white sets  $\tilde{\mathbb{X}}$  and  $\tilde{\mathbb{A}}^c$ .

to this obstacle, we adopt the framework introduced in [\[6\]](#) (see also [\[10, Chapter 10\]](#)). Here, the classical  $\mathcal{H}_2$  space is replaced by the space consisting of all the functions  $\mathbf{F}$  for which  $(\mathbf{F} \circ \psi(\cdot))\psi'(\cdot)^{\frac{1}{2}} \in \mathcal{H}_2$ , where  $\psi$  is a given conformal map. We generalize the definition of this space given in [\[6\]](#) for matrix valued functions.

**Definition 1** ( $\mathcal{H}_2(\bar{\mathbb{A}}^c)$  space, [\[6\]](#)). *Let  $\mathbf{F}: \bar{\mathbb{A}}^c \rightarrow \mathbb{C}^{q \times m}$  and  $\mathbf{H}: \bar{\mathbb{A}}^c \rightarrow \mathbb{C}^{q \times m}$  be analytic. Define*

$$\mathfrak{H}_{\mathbf{F}}(\cdot) = (\mathbf{F} \circ \psi(\cdot))\psi'(\cdot)^{\frac{1}{2}}. \quad (7)$$

Then the  $\mathcal{H}_2(\bar{\mathbb{A}}^c)$  inner product is defined as

$$\langle \mathbf{F}, \mathbf{H} \rangle_{\mathcal{H}_2(\bar{\mathbb{A}}^c)} := \langle \mathfrak{H}_{\mathbf{F}}, \mathfrak{H}_{\mathbf{H}} \rangle_{\mathcal{H}_2}$$

with the corresponding  $\mathcal{H}_2(\bar{\mathbb{A}}^c)$ -norm

$$\|\mathbf{F}\|_{\mathcal{H}_2(\bar{\mathbb{A}}^c)} := \|\mathfrak{H}_{\mathbf{F}}\|_{\mathcal{H}_2} = (\langle \mathfrak{H}_{\mathbf{F}}, \mathfrak{H}_{\mathbf{F}} \rangle_{\mathcal{H}_2})^{\frac{1}{2}}.$$

The space  $\mathcal{H}_2(\bar{\mathbb{A}}^c)$  is defined as

$$\mathcal{H}_2(\bar{\mathbb{A}}^c) := \left\{ \mathbf{F}: \bar{\mathbb{A}}^c \rightarrow \mathbb{C}^{q \times m} \text{ analytic} \mid \|\mathbf{F}\|_{\mathcal{H}_2(\bar{\mathbb{A}}^c)} < \infty \right\}.$$

[Definition 1](#) implies that if  $\mathbf{F} \in \mathcal{H}_2(\bar{\mathbb{A}}^c)$  then  $\mathfrak{H}_{\mathbf{F}} \in \mathcal{H}_2$ . Given the particular structure of an LTI system's transfer function  $\mathbf{G}$  as in [\(2\)](#), we write the corresponding operator  $\mathfrak{H}_{\mathbf{G}}$  as

$$\begin{aligned} \mathfrak{H}_{\mathbf{G}}(\cdot) &= (\mathbf{G} \circ \psi(\cdot))\psi'(\cdot)^{\frac{1}{2}} \\ &= \mathbf{C}(\psi(\cdot)\mathbf{I} - \mathbf{A})^{-1}\mathbf{B}\psi'(\cdot)^{\frac{1}{2}} \\ &= \mathbf{C}\mathbf{K}(\cdot)^{-1}\mathbf{B}, \end{aligned} \quad (8)$$

where

$$\mathbf{K}(\cdot) = \psi(\cdot)\psi'(\cdot)^{-\frac{1}{2}}\mathbf{I} - \mathbf{A}\psi'(\cdot)^{-\frac{1}{2}}. \quad (9)$$

### 2.3 Balanced truncation

In this section, we briefly review the concept of balanced truncation (BT) for asymptotically stable LTI systems with poles in  $\mathbb{A} = \mathbb{C}_-$ . BT is a (Petrov-Galerkin) projection-based model reduction technique. In other words, it constructs two model reduction bases  $\mathbf{V}_r \in \mathbb{C}^{n \times r}$  and  $\mathbf{W}_r \in \mathbb{C}^{n \times r}$  such that the state-space representation (system matrices) of the ROM in (3) is given by

$$\mathbf{A}_r = \mathbf{W}_r^* \mathbf{A} \mathbf{V}_r, \quad \mathbf{B}_r = \mathbf{W}_r^* \mathbf{B}, \quad \mathbf{C}_r = \mathbf{C} \mathbf{V}_r. \quad (10)$$

BT chooses  $\mathbf{V}_r$  and  $\mathbf{W}_r$  to eliminate hard-to-reach and hard-to-observe states of the original FOM in (1) [1, Section 7.1]. The computation of  $\mathbf{V}_r$  and  $\mathbf{W}_r$  depends on the controllability and observability Gramians of (1), denoted by  $\mathbf{X}_c$  and  $\mathbf{X}_o$ , respectively. For a minimal system, these Gramians are the symmetric positive definite unique solutions to the Lyapunov equations

$$\mathbf{A} \mathbf{X}_c + \mathbf{X}_c \mathbf{A}^* = -\mathbf{B} \mathbf{B}^*, \quad \mathbf{A}^* \mathbf{X}_o + \mathbf{X}_o \mathbf{A} = -\mathbf{C}^* \mathbf{C}. \quad (11)$$

The Gramians  $\mathbf{X}_c$  and  $\mathbf{X}_o$  given as the solutions to the Lyapunov equations (11) can be equivalently defined as integrals in the frequency domain, namely

$$\mathbf{X}_c = \frac{1}{2\pi} \int_{-\infty}^{\infty} (i\omega \mathbf{I} - \mathbf{A})^{-1} \mathbf{B} \mathbf{B}^* (i\omega \mathbf{I} - \mathbf{A})^{-*} d\omega, \quad (12)$$

$$\mathbf{X}_o = \frac{1}{2\pi} \int_{-\infty}^{\infty} (i\omega \mathbf{I} - \mathbf{A})^{-*} \mathbf{C}^* \mathbf{C} (i\omega \mathbf{I} - \mathbf{A})^{-1} d\omega. \quad (13)$$

These frequency domain definitions will play a crucial role in our development of BT via conformal maps in Section 3. In practice, one does not solve (11) for  $\mathbf{X}_c$  and  $\mathbf{X}_o$ . Instead one solves for their square-root factors. More precisely, let  $\mathbf{X}_c = \mathbf{U} \mathbf{U}^*$  and  $\mathbf{X}_o = \mathbf{L} \mathbf{L}^*$  be Cholesky decompositions. The existence of  $\mathbf{U}$  and  $\mathbf{L}$  is guaranteed via the positive definiteness of  $\mathbf{X}_c$  and  $\mathbf{X}_o$ . Then, one solves (11) directly for  $\mathbf{U}$  and  $\mathbf{L}$ . We refer the reader to [8] for details. Let

$$\mathbf{U}^* \mathbf{L} = \mathbf{Z} \mathbf{\Sigma} \mathbf{Y}^* = [\mathbf{Z}_r \quad \mathbf{Z}_2] \begin{bmatrix} \mathbf{\Sigma}_1 & \\ & \mathbf{\Sigma}_2 \end{bmatrix} \begin{bmatrix} \mathbf{Y}_r^* \\ \mathbf{Y}_2^* \end{bmatrix},$$

be the singular value decomposition where the entries of  $\mathbf{\Sigma}$  are called the Hankel singular values of the FOM. Here,  $\mathbf{\Sigma}_1 \in \mathbb{R}^{r \times r}$  contains the dominant  $r$  singular values, and  $\mathbf{Z}_r \in \mathbb{C}^{n \times r}$  and  $\mathbf{Y}_r \in \mathbb{C}^{n \times r}$  are corresponding left and right singular vectors. BT then constructs the model reduction matrices as  $\mathbf{W}_r = \mathbf{L} \mathbf{Y}_r \mathbf{S}_1^{-1/2}$  and  $\mathbf{V}_r = \mathbf{U} \mathbf{Z}_r \mathbf{S}_1^{-1/2}$ , which are then used to construct the matrices in (10) for the reduced system in (3).

ROM (3) via BT has important advantages. Firstly,  $\mathbf{G}_r$  in (4) is asymptotically stable and  $\|\mathbf{G} - \mathbf{G}_r\|_{\mathcal{H}_\infty} \leq 2 \text{trace}\{\mathbf{\Sigma}_2\}$ , where  $\|\mathbf{F}\|_{\mathcal{H}_\infty} := \sup_{\omega \in \mathbb{R}} \|\mathbf{F}(i\omega)\|_2$  denotes the  $\mathcal{H}_\infty$  norm (see also [1, Theorem 7.9]). Secondly, there also exists a bound on the  $\mathcal{H}_2$  error norm [1, Section 7.2.2]. We give a brief summary below. Consider the *balanced* realization of  $\mathbf{G}$  as  $\mathbf{G}(\cdot) = \mathbf{C}_B(\cdot \mathbf{I} - \mathbf{A}_B)^{-1} \mathbf{B}_B$ , i.e., a state-space realization of  $\mathbf{G}$  such that

$$\mathbf{X}_c = \mathbf{X}_o = \text{diag}(\sigma_1 \dots \sigma_n) = \begin{bmatrix} \mathbf{\Sigma}_1 & \\ & \mathbf{\Sigma}_2 \end{bmatrix}.$$

Let  $\mathbf{A}_B$  and  $\mathbf{B}_B$  be partitioned accordingly as

$$\mathbf{A}_B = \begin{bmatrix} \mathbf{A}_{11} & \mathbf{A}_{12} \\ \mathbf{A}_{21} & \mathbf{A}_{22} \end{bmatrix}, \quad \mathbf{B}_B = \begin{bmatrix} \mathbf{B}_1 \\ \mathbf{B}_2 \end{bmatrix},$$

and let

$$\mathbf{G}_2(\cdot) = \mathbf{A}_{12} \mathbf{\Sigma}_2 (\cdot \mathbf{I} - \mathbf{A}_{22} - \mathbf{A}_{21}(\cdot \mathbf{I} - \mathbf{A}_{11})^{-1} \mathbf{A}_{12})^{-1} \mathbf{\Sigma}_2 \mathbf{A}_{21}.$$

Then it holds

$$\|\mathbf{G} - \mathbf{G}_r\|_{\mathcal{H}_2}^2 \leq \text{trace}\{\mathbf{C}_2 \mathbf{\Sigma}_2 \mathbf{C}_2^*\} + 2\kappa \|\mathbf{G}_2\|_{\mathcal{H}_\infty},$$

for some  $\kappa \in \mathbb{R}$ . In Theorem 4 below, one of our main results, we utilize ideas from [18] for structured systems to derive an analogous bound for our BT via conformal mapping framework as well.

## 3 Balanced truncation with conformal maps

We now consider  $\mathbf{G} \in \mathcal{H}_2(\bar{\mathbb{A}}^c)$  structured as in (2) (with poles in  $\mathbb{A} \subset \mathbb{C}$ ) and extend the concept of BT to these systems. Since the Gramians are the main ingredient of BT, we first need to define them for  $\mathbf{G} \in \mathcal{H}_2(\bar{\mathbb{A}}^c)$ .

### 3.1 Defining the Gramians

For  $\mathbf{G} \in \mathcal{H}_2(\bar{\mathbb{A}}^c)$ , we recall that, for the conformally mapped function  $\mathfrak{H}_{\mathbf{G}}$  with its *state-space* representation as in (8), it holds that  $\mathfrak{H}_{\mathbf{G}} \in \mathcal{H}_2$ . Then, inspired by the frequency domain representation of the Gramians in (12) and (13) for the classical case of  $\mathbf{G}(\cdot) = \mathbf{C}(\cdot \mathbf{I} - \mathbf{A})^{-1} \mathbf{B}$  and by the Gramians defined for integro-differential equations in [7], we define the controllability and observability Gramians with respect to  $\mathfrak{H}_{\mathbf{G}}(\cdot) = \mathbf{C} \mathbf{K}(\cdot)^{-1} \mathbf{B}$  as

$$\mathbf{X}_c = \frac{1}{2\pi} \int_{-\infty}^{\infty} \mathbf{K}(i\omega)^{-1} \mathbf{B} \mathbf{B}^* \mathbf{K}(i\omega)^{-*} d\omega, \quad (14)$$

$$\mathbf{X}_o = \frac{1}{2\pi} \int_{-\infty}^{\infty} \mathbf{K}(i\omega)^{-*} \mathbf{C}^* \mathbf{C} \mathbf{K}(i\omega)^{-1} d\omega. \quad (15)$$

where  $\mathbf{K}(\cdot)$  is as defined in (9).

Unlike the classical BT case for asymptotically stable LTI systems where the Gramians can be computed as solutions to the Lyapunov equations (11), the newly defined Gramians in (14) and (15) cannot be obtained easily for general conformal maps  $\psi$ . In these general cases, one can compute an approximation of  $\mathbf{X}_c$  and  $\mathbf{X}_o$  through numerical quadrature. For example, the approximate controllability Gramian can be computed as

$$\mathbf{X}_c \approx \tilde{\mathbf{X}}_c = \sum_{j=1}^N w_j \mathbf{K}(ip_j)^{-1} \mathbf{B} \mathbf{B}^* \mathbf{K}(ip_j)^{-*}, \quad (16)$$

where  $w_j$  and  $p_j$  are the quadrature weights and nodes respectively. The observability Gramian can be approximated similarly. Even though the quadrature-based approximation (16) to the Gramians will be employed for general conformal maps, we will show in the next section, more specifically in Theorem 2, that for a particular type of conformal mapping, namely the Möbius transformation, the Gramians in (14) and (15) can still be computed by solving a modified Lyapunov equation.

### 3.2 Lyapunov equations

We start the section with a result on the uniqueness of the solution to a specific Lyapunov-like equation.

**Lemma 1** (Unique solution). *Consider the domains  $\mathbb{A} \subset \mathbb{C}$  and  $\mathbb{X} \subseteq \mathbb{C}_-$ . Let the matrix  $\mathbf{A} \in \mathbb{C}^{n \times n}$  have the eigendecomposition  $\mathbf{A} = \mathbf{V} \mathbf{\Lambda} \mathbf{V}^{-1}$ , with  $\mathbf{\Lambda} = \text{diag}(\lambda_1, \dots, \lambda_n)$ , and  $\lambda_j \in \mathbb{A}$ , for  $j = 1, \dots, n$ , are distinct. Let  $f: \mathbb{A} \rightarrow \mathbb{X}$  be analytic. Then the Lyapunov equation*

$$f(\mathbf{A}) \mathbf{P} + \mathbf{P} f(\mathbf{A})^* = \mathbf{Q}, \quad (17)$$

with  $\mathbf{Q} = \mathbf{Q}^* \in \mathbb{C}^{n \times n}$ , has a unique solution  $\mathbf{P}$ .

*Proof.* The main idea behind this result is the fact that the Sylvester equation

$$\mathbf{Z} \mathbf{P} + \mathbf{P} \mathbf{Y} = \mathbf{Q},$$

where  $\mathbf{Z} \in \mathbb{C}^{n_Z \times n_Z}$ ,  $\mathbf{Y} \in \mathbb{C}^{n_Y \times n_Y}$ ,  $\mathbf{Q} \in \mathbb{C}^{n_Z \times n_Y}$ , has a unique solution  $\mathbf{P} \in \mathbb{C}^{n_Z \times n_Y}$  if and only if  $\mathbf{Z}$  and  $-\mathbf{Y}$  do not share any eigenvalues (see [1, Proposition 6.2]). In our case we have  $\mathbf{Z} = f(\mathbf{A})$  and  $\mathbf{Y} = f(\mathbf{A})^*$ . Given the eigendecomposition of  $\mathbf{A}$ , we can then write

$$f(\mathbf{A}) = \mathbf{V} f(\mathbf{\Lambda}) \mathbf{V}^{-1} = \mathbf{V} \begin{bmatrix} f(\lambda_1) & & \\ & \ddots & \\ & & f(\lambda_n) \end{bmatrix} \mathbf{V}^{-1}, \quad (18)$$

(see also [13, Definition 1.2]). Since  $\mathbf{\Lambda} \in \mathbb{A}$  we have that  $f(\mathbf{\Lambda}) \in \mathbb{X}$  with  $\mathbb{X} \subseteq \mathbb{C}_-$ . Given that the eigenvalues of  $f(\mathbf{A})$

are the mirror images of the eigenvalues of  $-f(\mathbf{A})^*$  with respect to the imaginary axis, then, the two matrices  $f(\mathbf{A})$  and  $-f(\mathbf{A})^*$  do not share any eigenvalues and thus (17) has a unique solution.  $\square$

**Remark 1.** *One can prove Lemma 1 without the diagonalizability (and the simple eigenvalues) assumption on  $\mathbf{A}$ . It is avoided here since the notation and presentation becomes rather cumbersome. Next we briefly explain how the argument goes in that case. Let  $\mathbf{A} = \mathbf{U} \mathbf{T} \mathbf{U}^*$  be the Schur decomposition of  $\mathbf{A}$  where  $\mathbf{U}$  is a unitary matrix and  $\mathbf{T}$  is an upper triangular matrix. The computation of the matrix function  $f(\mathbf{A})$  in (18) can then be carried out, e.g., following the approach discussed in [9]. Applying [9, Algorithm 5.1] results in  $f(\mathbf{A}) = \mathbf{F} = \mathbf{U} \mathbf{N} \mathbf{U}^*$  where  $\mathbf{N}$  is an upper triangular matrix with  $f(\lambda_i)$ ,  $i = 1, \dots, n$  as the diagonal entries. Since  $\mathbf{N}$  and  $\mathbf{F}$  are similar, the eigenvalues of  $\mathbf{F}$  are given by  $f(\lambda_i)$  for  $i = 1, \dots, n$  which, then, would allow to apply similar arguments as in the proof of Lemma 1.*

We now show that the newly defined Gramians in (14) and (15) for  $\mathfrak{H}_{\mathbf{G}}$  in (8) solve (modified) Lyapunov equations of the form (17) when the Möbius transformation is adopted in the mapping from  $\mathbf{G}$  to  $\mathfrak{H}_{\mathbf{G}}$ .

**Theorem 2.** *Consider the transfer function  $\mathbf{G} \in \mathcal{H}_2(\bar{\mathbb{A}}^c)$  with poles  $\lambda_j \in \mathbb{A}$ ,  $j = 1, \dots, n$ , and the Möbius transformation  $m(\cdot) = (\alpha \cdot + \beta) / (\gamma \cdot + \delta)$  in (5) such that  $m: \mathbb{C}_- \rightarrow \mathbb{A}$  and  $m: i\mathbb{R} \rightarrow \partial\mathbb{A}^+$ . Then the controllability and observability Gramians  $\mathbf{X}_c, \mathbf{X}_o$  in (14) and (15) are the unique solutions of the Lyapunov equations*

$$m^{-1}(\mathbf{A}) \mathbf{X}_c + \mathbf{X}_c m^{-1}(\mathbf{A})^* = -\mathbf{Q}_c, \quad \text{and} \quad (19)$$

$$\mathbf{X}_o m^{-1}(\mathbf{A}) + m^{-1}(\mathbf{A})^* \mathbf{X}_o = -\mathbf{Q}_o, \quad (20)$$

where  $m^{-1}(\mathbf{A})$  is defined as in (6), and

$$\mathbf{Q}_c = |\alpha\delta - \beta\gamma| (\alpha \mathbf{I} - \gamma \mathbf{A})^{-1} \mathbf{B} \mathbf{B}^* (\alpha \mathbf{I} - \gamma \mathbf{A})^{-*},$$

$$\mathbf{Q}_o = |\alpha\delta - \beta\gamma| (\alpha \mathbf{I} - \gamma \mathbf{A})^{-*} \mathbf{C}^* \mathbf{C} (\alpha \mathbf{I} - \gamma \mathbf{A})^{-1}.$$

*Proof.* We first focus on the controllability Gramian. For the specific mapping  $m$ , the Gramian in (14) is given by

$$\mathbf{X}_c = \frac{1}{2\pi} \int_{-\infty}^{\infty} (m(i\omega) \mathbf{I} - \mathbf{A})^{-1} \mathbf{B} \left( m'(i\omega)^{1/2} \right) \left( m'(i\omega)^{1/2} \right)^* \mathbf{B}^* (m(i\omega) \mathbf{I} - \mathbf{A})^{-*} d\omega,$$

where

$$m'(\cdot) = \frac{\alpha\delta - \beta\gamma}{(\gamma \cdot + \delta)^2},$$

is the derivative of  $m$ . We then obtain

$$\begin{aligned} \mathbf{X}_c &= \\ &= \frac{1}{2\pi} \int_{-\infty}^{\infty} (m(i\omega)\mathbf{I} - \mathbf{A})^{-1} \mathbf{B} \frac{|\alpha\delta - \beta\gamma|}{(\gamma i\omega + \delta)(\gamma i\omega + \delta)^*} \\ &\quad \mathbf{B}^* (m(i\omega)\mathbf{I} - \mathbf{A})^{-*} d\omega \\ &= \frac{1}{2\pi} \int_{-\infty}^{\infty} \mathbf{R}(i\omega)^{-1} \mathbf{B} \mathbf{B}^* \mathbf{R}(i\omega)^{-*} |\alpha\delta - \beta\gamma| d\omega, \end{aligned} \quad (21)$$

where  $\mathbf{R}(\cdot)^{-1} = ((\alpha\cdot + \beta)\mathbf{I} - (\gamma\cdot + \delta)\mathbf{A})^{-1}$ . We rewrite  $\mathbf{R}(\cdot)^{-1}$  using the manipulations

$$\begin{aligned} \mathbf{R}(\cdot)^{-1} &= ((\alpha\mathbf{I} - \gamma\mathbf{A}) + \beta\mathbf{I} - \delta\mathbf{A})^{-1} \\ &= (\mathbf{I} - (\beta\mathbf{I} - \delta\mathbf{A})(\gamma\mathbf{A} - \alpha\mathbf{I})^{-1})^{-1} (\alpha\mathbf{I} - \gamma\mathbf{A})^{-1} \\ &= (\mathbf{I} - m^{-1}(\mathbf{A}))^{-1} (\alpha\mathbf{I} - \gamma\mathbf{A})^{-1}. \end{aligned} \quad (22)$$

Define  $\mathbf{Q}_c = |\alpha\delta - \beta\gamma|(\alpha\mathbf{I} - \gamma\mathbf{A})^{-1} \mathbf{B} \mathbf{B}^* (\alpha\mathbf{I} - \gamma\mathbf{A})^{-*}$ . Then, using (22) in (21), the Gramian  $\mathbf{X}_c$  becomes

$$\mathbf{X}_c = \frac{1}{2\pi} \int_{-\infty}^{\infty} (i\omega\mathbf{I} - m^{-1}(\mathbf{A}))^{-1} \mathbf{Q}_c (i\omega\mathbf{I} - m^{-1}(\mathbf{A}))^{-*} d\omega.$$

Applying Plancherel's theorem results in

$$\mathbf{X}_c = \int_0^{\infty} e^{m^{-1}(\mathbf{A})t} \mathbf{Q}_c e^{m^{-1}(\mathbf{A})^*t} dt. \quad (23)$$

Since  $m: \mathbb{C}_- \rightarrow \mathbb{A}$ , the eigenvalues of  $m^{-1}(\mathbf{A})$  are in the open left-half complex plane so that the exponential term in (23) vanishes for  $t \rightarrow \infty$ . As in the standard case, we therefore obtain

$$\begin{aligned} m^{-1}(\mathbf{A})\mathbf{X}_c + \mathbf{X}_c m^{-1}(\mathbf{A})^* &= \\ &= \int_0^{\infty} \frac{d}{dt} e^{m^{-1}(\mathbf{A})t} \mathbf{Q}_c e^{m^{-1}(\mathbf{A})^*t} dt = -\mathbf{Q}_c, \end{aligned}$$

which is the Lyapunov equation (19). Since  $m^{-1}: \mathbb{A} \rightarrow \mathbb{C}_-$ , the uniqueness of  $\mathbf{X}_c$  follows from Lemma 1. Similar arguments apply to prove (20).  $\square$

We now have all the tools to develop the conformal BT algorithm that handles systems with transfer functions of the kind  $\mathbf{G} \in \mathcal{H}_2(\bar{\mathbb{A}}^c)$ . In Algorithm 1 we provide a pseudocode of the proposed algorithm, called `conformalBT`. The major difference from classical BT is that the Gramians are defined (via the conformal mapping) with respect to  $\mathfrak{H}_{\mathbf{G}}$  and not  $\mathbf{G}$  (see (14) and (15)). However, the resulting projection matrices are then applied directly to the system matrices of the original system  $\mathbf{G}$  and not  $\mathfrak{H}_{\mathbf{G}}$ . After studying the theoretical properties of `conformalBT` in the next section, we will illustrate its performance numerically in Section 5. We note that the pseudocode first computes the Gramians and

then the Cholesky factors in order to keep the presentation to align with the analytical development. In practice one would compute the (approximate) Cholesky factors directly without ever forming  $\mathbf{X}_c$  and  $\mathbf{X}_o$ .

---

**Algorithm 1** Conformal balanced truncation (`conformalBT`)

---

**Input:** FOM  $(\mathbf{A}, \mathbf{B}, \mathbf{C})$ , conformal map  $\psi$ , reduced order  $r < n$

- 1: **if**  $\psi$  is a Möbius transformation as in Theorem 2 **then**
- 2:   Solve (19) and (20) to get  $\mathbf{X}_c$  and  $\mathbf{X}_o$
- 3: **else**
- 4:   Compute  $\mathbf{X}_c$  and  $\mathbf{X}_o$  by approximating (14) and (15)
- 5: **end**
- 6: Compute Cholesky factorizations  $\mathbf{X}_c = \mathbf{U}\mathbf{U}^*$  and  $\mathbf{X}_o = \mathbf{L}\mathbf{L}^*$
- 7: Compute SVD of  $\mathbf{U}^*\mathbf{L}$  and partition it as follows

$$\mathbf{U}^*\mathbf{L} = [\mathbf{Z}_r \quad \mathbf{Z}_2] \begin{bmatrix} \Sigma_1 & \\ & \Sigma_2 \end{bmatrix} \begin{bmatrix} \mathbf{Y}_r^* \\ \mathbf{Y}_2^* \end{bmatrix}$$

- 8: Compute  $\mathbf{W}_r = \mathbf{L}\mathbf{Y}_r^* \Sigma_1^{-1/2}$ ,  $\mathbf{V}_r = \mathbf{U}\mathbf{Z}_r \Sigma_1^{-1/2}$
- 9: Compute the reduced system matrices

$$\mathbf{A}_r = \mathbf{W}_r^* \mathbf{A} \mathbf{V}_r, \quad \mathbf{B}_r = \mathbf{W}_r^* \mathbf{B}, \quad \mathbf{C}_r = \mathbf{C} \mathbf{V}_r$$

10: **return**  $\mathbf{A}_r, \mathbf{B}_r, \mathbf{C}_r$

---

## 4 Stability preservation and $\mathcal{H}_2$ error bound

In this section, we discuss properties of reduced models obtained by Algorithm 1. In particular, for the specific case of a Möbius transformation, we show preservation of stability and for the general case, we discuss an  $\mathcal{H}_2$ -type error bound. We begin by relating the range of a specific Möbius transformation to a Hermitian polynomial.

**Lemma 2.** Consider the Möbius transformation (5) such that  $m: \mathbb{C}_- \rightarrow \mathbb{A}$  with pole on the right half plane. Define the polynomial  $h$  as

$$h(z) = \begin{bmatrix} 1 & z \end{bmatrix} \begin{bmatrix} \beta\alpha^* + \beta^*\alpha & (-\delta\alpha^* - \gamma\beta^*)^* \\ -\delta\alpha^* - \gamma\beta^* & \delta\gamma^* + \delta^*\gamma \end{bmatrix} \begin{bmatrix} 1 \\ z^* \end{bmatrix}.$$

Then it holds that

$$\mathbb{S} := \{z \in \mathbb{C} \mid h(z) > 0\} = \mathbb{A}.$$

*Proof.* “ $\subseteq$ ” Consider  $z \in \mathbb{S}$ . Note that we may also consider  $m$  as a bijective mapping from  $\mathbb{C} \setminus \{-\frac{\delta}{\gamma}\}$  to  $\mathbb{C} \setminus \{\frac{\alpha}{\gamma}\}$ , see (5).

Let us now first assume that  $z \neq \frac{\alpha}{\gamma}$ . Then there exists  $s \in \mathbb{C} \setminus \{-\frac{\delta}{\gamma}\}$  such that  $z = m(s)$ . Utilizing the specific form of  $m$  in (5) yields

$$h(z) = h(m(s)) = -\frac{|\alpha\delta - \beta\gamma|^2}{|\gamma s + \delta|^2} (s + s^*) > 0. \quad (24)$$

This implies that  $s + s^* = 2\text{Re}\{s\} < 0$ , i.e.,  $s \in \mathbb{C}_-$ . On the other hand, for  $z = \frac{\alpha}{\gamma}$  we have the equality  $h(\frac{\alpha}{\gamma}) = 0$ , which contradicts  $h(z) > 0$ . Hence, it follows that  $z = m(s) \in \mathbb{A}$  and therefore  $\mathbb{S} \subseteq \mathbb{A}$ .

“ $\supseteq$ ” Consider  $z \in \mathbb{A}$ . Then, since  $m$  as a mapping from  $\mathbb{C}_-$  to  $\mathbb{A}$  is surjective, there exists  $s \in \mathbb{C}_-$  with  $m(s) = z$ . Now as in (24) consider the explicit expression for  $h(m(s))$ . Note that  $\gamma s + \delta \neq 0$  since  $s \in \mathbb{C}_-$  and we assumed  $m$  to have its pole in the right half plane. Moreover, since  $\text{Re}\{s\} < 0$  and  $|\alpha\delta - \beta\gamma|^2/|\gamma s + \delta|^2 > 0$ , we have that  $h(z) = h(m(s)) > 0$ . This shows  $\mathbb{A} \subseteq \mathbb{S}$ ; and so  $\mathbb{S} = \mathbb{A}$ .  $\square$

In the generic case of  $\mathbb{A} = \mathbb{C}_-$ , i.e., in the case of asymptotically stable systems with poles in the open left-half plane, BT retains asymptotic stability. The situation is rather different in `conformalBT` since (i) the balanced system  $\mathfrak{H}_{\mathbf{G}}$  (8) does not have the generic first-order state-space form and (ii) the reduction is applied on the original state-space quantities of  $\mathbf{G}$  (as in Step 9 of Algorithm 1) not of  $\mathfrak{H}_{\mathbf{G}}$ . When does `conformalBT` preserve stability in the sense that the retained poles also lie in the set  $\mathbb{A}$ ? Below we prove this stability preservation result for `conformalBT` when specific Möbius transformations are adopted as conformal maps. Before we state the result, we recall that a *balanced* system has equal and diagonal Gramians. Thus in the setting of `conformalBT`,  $\mathbf{G}$  is *conformally balanced* means that the Gramians (of  $\mathfrak{H}_{\mathbf{G}}$ ) defined in (14) and (15) are equal and diagonal. In addition, when we refer to a *controllable* system we mean that the controllability matrix of  $\mathbf{G}$  is full rank.

**Theorem 3.** *Let the system  $\mathbf{G} \in \mathcal{H}_2(\bar{\mathbb{A}}^c)$  with poles in the open set  $\mathbb{A}$  be controllable. Also let the Möbius transformation (5) parametrized as in Theorem 2 with a pole in the right half plane or  $\gamma = 0$ , be employed in `conformalBT`. Choose  $r$  in Step 7 of Algorithm 1 such that  $\Sigma_1$  is positive definite and has no diagonal entries in common with  $\Sigma_2$ . Then the reduced system resulting from `conformalBT` will have its poles in the open set  $\mathbb{A}$ .*

*Proof.* Let  $\mathbf{X}_c$  and  $\mathbf{X}_o$  be the solutions to the Lyapunov equations (19) and (20), respectively. We start by inserting the formula for the matrix function  $m^{-1}(\mathbf{A}) = (\beta\mathbf{I} - \delta\mathbf{A})(\gamma\mathbf{A} - \alpha\mathbf{I})^{-1}$  into (19) to obtain

$$\begin{aligned} (\beta\mathbf{I} - \delta\mathbf{A})(\gamma\mathbf{A} - \alpha\mathbf{I})^{-1}\mathbf{X}_c + \mathbf{X}_c(\gamma\mathbf{A} - \alpha\mathbf{I})^{-*}(\beta\mathbf{I} - \delta\mathbf{A})^* \\ = -|\alpha\delta - \beta\gamma|(\alpha\mathbf{I} - \gamma\mathbf{A})^{-1}\mathbf{B}\mathbf{B}^*(\alpha\mathbf{I} - \gamma\mathbf{A})^{-*}. \end{aligned}$$

Using the fact that the two matrices  $(\beta\mathbf{I} - \delta\mathbf{A})$  and  $(\gamma\mathbf{A} - \alpha\mathbf{I})^{-1}$  commute, we obtain

$$\begin{aligned} -(\beta\mathbf{I} - \delta\mathbf{A})\mathbf{X}_c(\gamma\mathbf{A} - \alpha\mathbf{I})^* - (\gamma\mathbf{A} - \alpha\mathbf{I})\mathbf{X}_c(\beta\mathbf{I} - \delta\mathbf{A})^* \\ = -|\alpha\delta - \beta\gamma|\mathbf{B}\mathbf{B}^*, \end{aligned}$$

which results in

$$\kappa_1\mathbf{A}\mathbf{X}_c\mathbf{A}^* + \kappa_2\mathbf{X}_c + \kappa_3\mathbf{A}\mathbf{X}_c + \kappa_3^*\mathbf{X}_c\mathbf{A}^* = -|\alpha\delta - \beta\gamma|\mathbf{B}\mathbf{B}^*, \quad (25)$$

with

$$\kappa_1 = -\gamma^*\delta - \gamma\delta^*, \quad \kappa_2 = -\alpha^*\beta - \alpha\beta^*, \quad \kappa_3 = \alpha^*\delta + \beta^*\gamma.$$

Without loss of generality we assume  $\mathbf{G}(\cdot) = \mathbf{C}_{\mathbf{B}}(\cdot\mathbf{I} - \mathbf{A}_{\mathbf{B}})^{-1}\mathbf{B}_{\mathbf{B}}$  is (conformally) balanced, i.e.,

$$\mathbf{X}_c = \mathbf{X}_o = \Sigma = \begin{bmatrix} \Sigma_1 & \\ & \Sigma_2 \end{bmatrix},$$

with  $\Sigma$  being a diagonal matrix. In addition, we partition the balanced system matrices as follows

$$\mathbf{A}_{\mathbf{B}} = \begin{bmatrix} \mathbf{A}_r & \mathbf{A}_{12} \\ \mathbf{A}_{21} & \mathbf{A}_{22} \end{bmatrix}, \quad \mathbf{C}_{\mathbf{B}} = [\mathbf{C}_r \quad \mathbf{C}_2], \quad \mathbf{B}_{\mathbf{B}} = \begin{bmatrix} \mathbf{B}_r \\ \mathbf{B}_2 \end{bmatrix}. \quad (26)$$

After substituting the balanced system into (25) we consider the first row and column block equation to obtain

$$\begin{aligned} \kappa_1(\mathbf{A}_r\Sigma_1\mathbf{A}_r^* + \mathbf{A}_{12}\Sigma_2\mathbf{A}_{12}^*) + \kappa_2\Sigma_1 + \kappa_3\mathbf{A}_r\Sigma_1 + \kappa_3^*\Sigma_1\mathbf{A}_r^* \\ = -|\alpha\delta - \beta\gamma|\mathbf{B}_r\mathbf{B}_r^*. \end{aligned}$$

We now adopt a similar strategy to [1, Section 7.2.1]. Let  $\mathbf{A}_r^*\mathbf{v} = \mu\mathbf{v}$  and  $\mathbf{A}_r\mathbf{x} = \lambda\mathbf{x}$  with  $\lambda = \mu^*$  where  $\mathbf{v}$  and  $\mathbf{x}$  are the left- and right-eigenvectors of  $\mathbf{A}_r$  corresponding to the eigenvalue  $\lambda$ . Our goal is to show that  $\lambda \in \mathbb{A}$ . We multiply the last equation by  $\mathbf{v}^*$  and  $\mathbf{v}$  from the left and right, respectively to obtain

$$\begin{aligned} \kappa_1(\mu^*\mathbf{v}^*\Sigma_1\mathbf{v}\mu + \mathbf{v}^*\mathbf{A}_{12}\Sigma_2\mathbf{A}_{12}^*\mathbf{v}) + \kappa_2\mathbf{v}^*\Sigma_1\mathbf{v} + \kappa_3\mu^*\mathbf{v}^*\Sigma_1\mathbf{v} \\ + \kappa_3^*\mathbf{v}^*\Sigma_1\mathbf{v}\mu = -|\alpha\delta - \beta\gamma|\mathbf{v}^*\mathbf{B}_r\mathbf{B}_r^*\mathbf{v}, \end{aligned}$$

which becomes

$$\begin{aligned} (-\kappa_1|\mu|^2 - \kappa_3\mu^* - \kappa_3^*\mu - \kappa_2)\mathbf{v}^*\Sigma_1\mathbf{v} \\ = \kappa_1\mathbf{v}^*\mathbf{A}_{12}\Sigma_2\mathbf{A}_{12}^*\mathbf{v} + |\alpha\delta - \beta\gamma|\mathbf{v}^*\mathbf{B}_r\mathbf{B}_r^*\mathbf{v}. \end{aligned}$$

Let us first consider the case in which the Möbius transformation  $m$ , given in (5), has a finite pole in  $-\delta/\gamma$ , which can be written as

$$-\frac{\delta}{\gamma} = -\frac{\delta\gamma^*}{|\gamma|^2} = -\frac{\text{Re}\{\delta\gamma^*\}}{|\gamma|^2} - i\frac{\text{Im}\{\delta\gamma^*\}}{|\gamma|^2}.$$

We assumed that the pole of  $m$  lies in  $\mathbb{C}_+$ , which translates to having  $\operatorname{Re}\{\delta\gamma^*\} < 0$ . This results in

$$\kappa_1 = -\delta\gamma^* - \delta^*\gamma = -2\operatorname{Re}\{\delta\gamma^*\} > 0.$$

Because the terms  $\mathbf{A}_{12}\Sigma_2\mathbf{A}_{12}^*$  and  $\mathbf{B}_r\mathbf{B}_r^*$  are positive semi-definite we then get

$$\begin{aligned} & (-\kappa_1|\mu|^2 - \kappa_3\mu^* - \kappa_3^*\mu - \kappa_2)\mathbf{v}^*\Sigma_1\mathbf{v} \\ & = \kappa_1\mathbf{v}^*\mathbf{A}_{12}\Sigma_2\mathbf{A}_{12}^*\mathbf{v} + |\alpha\delta - \beta\gamma|\mathbf{v}^*\mathbf{B}_r\mathbf{B}_r^*\mathbf{v} \geq 0. \end{aligned}$$

The fact that  $\Sigma_1$  is positive definite implies

$$-\kappa_1|\mu|^2 - \kappa_3\mu^* - \kappa_3^*\mu - \kappa_2 \geq 0$$

After replacing  $\mu$  with  $\lambda^*$  we get

$$-\kappa_1|\lambda|^2 - \kappa_3^*\lambda^* - \kappa_3\lambda - \kappa_2 \geq 0. \quad (27)$$

To prove that the inequality in (27) is strict (so that we can employ Lemma 2) we consider the case

$$-\kappa_1|\lambda|^2 - \kappa_3^*\lambda^* - \kappa_3\lambda - \kappa_2 = 0.$$

Recall that  $\mathbf{A}_{12}\Sigma_2\mathbf{A}_{12}^*$  and  $\mathbf{B}_r\mathbf{B}_r^*$  are positive semi-definite, and  $\kappa_1 > 0$ . For the equality to hold, we then have  $\mathbf{v}^*\mathbf{A}_{12} = 0$  and  $\mathbf{v}^*\mathbf{B}_r = 0$ . Because  $\mathbf{v}^*$  is also a left eigenvector of  $\mathbf{A}_r$  then  $[\mathbf{v}^* \ 0]$  is a left eigenvector of  $\mathbf{A}_B$ . Due to  $[\mathbf{v}^* \ 0]$  being a non-trivial element of the left kernel of  $\mathbf{B}_B$  then the controllability matrix

$$[\mathbf{B}_B \ \mathbf{A}_B\mathbf{B}_B \ \dots \ \mathbf{A}_B^{n-1}\mathbf{B}_B],$$

does not have full rank. This results in the system not being controllable which contradicts the assumption of the theorem. In other words

$$-\kappa_1|\lambda|^2 - \kappa_3^*\lambda^* - \kappa_3\lambda - \kappa_2 > 0. \quad (28)$$

Due to Lemma 2 we can then conclude that the ROM poles need to be in  $\mathbb{A}$ .

The case of  $\gamma = 0$  needs some special care. First, we note that  $m: \mathbb{C} \rightarrow \mathbb{C}$  with  $m(s) = \frac{\alpha s + \beta}{\delta}$  is bijective and we obtain

$$\kappa_1 = 0, \ \kappa_2 = -\alpha^*\beta - \alpha\beta^*, \ \kappa_3 = \alpha^*\delta.$$

Then (25) becomes

$$\kappa_2\mathbf{X}_c + \kappa_3\mathbf{A}\mathbf{X}_c + \kappa_3^*\mathbf{X}_c\mathbf{A}^* = -|\alpha\delta|\mathbf{B}\mathbf{B}^*.$$

As above we consider the balanced realization of  $\mathbf{G}$  with matrices in (26) resulting in

$$\kappa_2\Sigma + \kappa_3\mathbf{A}_B\Sigma + \kappa_3^*\Sigma\mathbf{A}_B^* = -|\alpha\delta|\mathbf{B}_B\mathbf{B}_B^*.$$

Expanding the terms leads to

$$(\alpha^*\delta\mathbf{A}_B - \alpha^*\beta\mathbf{I})\Sigma + \Sigma(\alpha^*\delta\mathbf{A}_B - \alpha^*\beta\mathbf{I})^* = -|\alpha\delta|\mathbf{B}_B\mathbf{B}_B^*. \quad (29)$$

By multiplying the left and right hand side of (29) by  $|\alpha|^{-2}$  we can rewrite the equality as

$$\tilde{\mathbf{A}}_B\Sigma + \Sigma\tilde{\mathbf{A}}_B^* = -\frac{|\alpha\delta|}{|\alpha|^2}\mathbf{B}_B\mathbf{B}_B^*,$$

where  $\tilde{\mathbf{A}}_B = (\delta\mathbf{A}_B - \beta\mathbf{I})\alpha^{-1} = m^{-1}(\mathbf{A}_B)$ . Here,  $m^{-1}$  maps the spectrum of  $\mathbf{A}_B$  from  $\mathbb{A}$  into  $\mathbb{C}_-$ . Since  $\gamma = 0$ ,  $\tilde{\mathbf{A}}_B$  is a combination of scaling, rotation, and translation of the original matrix  $\mathbf{A}_B$ . Consider now the Krylov space spanned by the columns of the controllability matrix

$$\mathcal{K}(\mathbf{B}_B, \mathbf{A}_B) = \operatorname{span}\{\mathbf{B}_B, \mathbf{A}_B\mathbf{B}_B, \dots, \mathbf{A}_B^{n-1}\mathbf{B}_B\}.$$

Due to the system  $\mathbf{G}$  being controllable, we have that  $\mathcal{K}(\mathbf{B}_B, \mathbf{A}_B)$  spans  $\mathbb{C}^n$ . It is known that a Krylov space is invariant to scaling (including rotation) and translation. For this reason we have that  $\mathcal{K}(\frac{\sqrt{\alpha\delta}}{\alpha}\mathbf{B}_B, \tilde{\mathbf{A}}_B) = \mathcal{K}(\mathbf{B}_B, \mathbf{A}_B)$  which results in the system composed of the matrices  $(\tilde{\mathbf{A}}_B, \frac{\sqrt{\alpha\delta}}{\alpha}\mathbf{B}_B, \frac{\sqrt{\alpha\delta}}{\alpha}\mathbf{C}_B)$  being controllable. Now, consider the partition

$$\tilde{\mathbf{A}}_B = \begin{bmatrix} \tilde{\mathbf{A}}_r & \tilde{\mathbf{A}}_{12} \\ \tilde{\mathbf{A}}_{21} & \tilde{\mathbf{A}}_{22} \end{bmatrix},$$

we can then prove that the eigenvalues of  $\tilde{\mathbf{A}}_r$  lie in  $\mathbb{C}_-$  by simply following the proof in [1, Section 7.2.1] for the continuous-time case with a system having the matrices  $(\tilde{\mathbf{A}}_B, \frac{\sqrt{\alpha\delta}}{\alpha}\mathbf{B}_B, \frac{\sqrt{\alpha\delta}}{\alpha}\mathbf{C}_B)$ . Let  $\tilde{\lambda}$  and  $\lambda$  be eigenvalues of  $\tilde{\mathbf{A}}_r$  and  $\mathbf{A}_r$ , respectively. Due to  $\operatorname{Re}\{\tilde{\lambda}\} < 0$ , we then have that

$$\operatorname{Re}\{\tilde{\lambda}\} = \operatorname{Re}\left\{\frac{\delta\lambda - \beta}{\alpha}\right\} = \operatorname{Re}\{m^{-1}(\lambda)\} < 0. \quad (30)$$

Due to the bijectivity of  $m^{-1}$ , the only points that satisfy the inequality in (30) are  $\lambda \in \mathbb{A}$ .  $\square$

It is important to recall that even if the adopted Gramians are from  $\mathfrak{H}_{\mathbf{G}}$ , the theorem applies to the poles of the original system  $\mathbf{G}$  and not of  $\mathfrak{H}_{\mathbf{G}}$ . In Section 5 we illustrate how Theorem 3 applies (and is employed) in two numerical examples.

**Remark 2.** *It is important to note that we use the term stability in the sense described in [14, Section 3.4.7] and not necessarily meaning that the reduced system is asymptotically stable. More precisely, we adopt the term to indicate that if the full order system has its poles in a specific domain  $\mathbb{A}$  then the reduced model will have them in the same domain. If asymptotic stability needs to be achieved then it is essential to choose an appropriate conformal map with range in  $\mathbb{C}_-$ .*



The next theorem provides a bound for the error norm  $\|\mathbf{G} - \mathbf{G}_r\|_{\mathcal{H}_2(\bar{\mathbb{A}}^c)}$ , which directly results from [18] where general structured transfer functions are discussed. It is worth mentioning that, in what follows, we do not impose a specific conformal map to be used.

**Theorem 4.** *Given  $\mathbf{G} \in \mathcal{H}_2(\bar{\mathbb{A}}^c)$ , the reduced system  $\mathbf{G}_r$  from conformalBT satisfies the inequality*

$$\|\mathbf{G} - \mathbf{G}_r\|_{\mathcal{H}_2(\bar{\mathbb{A}}^c)}^2 \leq \text{trace}\{\mathbf{C}_2 \boldsymbol{\Sigma}_2 \mathbf{C}_2^*\} + \varepsilon \text{trace}\{\boldsymbol{\Sigma}_2\}, \quad (31)$$

where  $\varepsilon \in \mathbb{R}$  is a constant that depends on the (conformally) balanced realization of  $\mathbf{G}$  and  $\mathbf{G}_r$ , and  $\boldsymbol{\Sigma}_2$  indicates the neglected singular values in Step 7 of Algorithm 1.

*Proof.* The proof is similar to [18, Section 4.3.3]. Here we highlight the most important steps considering complex valued transfer functions. Consider the balanced realization  $\mathfrak{H}_{\mathbf{G}}(\cdot) = \mathbf{C}_{\mathcal{B}} \mathbf{K}_{\mathcal{B}}(\cdot)^{-1} \mathbf{B}_{\mathcal{B}}$  and let  $\mathbf{N}_{\mathcal{B}}(\cdot) = \mathbf{K}_{\mathcal{B}}(\cdot)^{-1} \mathbf{B}_{\mathcal{B}}$ . We then rewrite the controllability Gramian of  $\mathfrak{H}_{\mathbf{G}}$  from (8) as

$$\mathbf{X}_c = \frac{1}{2\pi} \int_{-\infty}^{\infty} \mathbf{N}(i\omega) \mathbf{N}(i\omega)^* d\omega = \underbrace{\begin{bmatrix} \boldsymbol{\Sigma}_1 & \\ & \boldsymbol{\Sigma}_2 \end{bmatrix}}_{\boldsymbol{\Sigma}}. \quad (32)$$

We then make the following partitions:

$$\begin{aligned} \mathbf{K}_{\mathcal{B}}(\cdot) &= \begin{bmatrix} \mathbf{K}_r(\cdot) & \mathbf{K}_{12}(\cdot) \\ \mathbf{K}_{21}(\cdot) & \mathbf{K}_{22}(\cdot) \end{bmatrix}, & \mathbf{C}_{\mathcal{B}} &= [\mathbf{C}_r \quad \mathbf{C}_2], \\ \mathbf{B}_{\mathcal{B}} &= \begin{bmatrix} \mathbf{B}_r \\ \mathbf{B}_2 \end{bmatrix}, & \mathbf{N}_{\mathcal{B}}(\cdot) &= \begin{bmatrix} \mathbf{N}_{\mathcal{B}1}(\cdot) \\ \mathbf{N}_{\mathcal{B}2}(\cdot) \end{bmatrix}. \end{aligned} \quad (33)$$

By inserting (33) into (32) we obtain

$$\begin{aligned} \boldsymbol{\Sigma}_1 &= \frac{1}{2\pi} \int_{-\infty}^{\infty} \mathbf{N}_{\mathcal{B}1}(i\omega) \mathbf{N}_{\mathcal{B}1}(i\omega)^* d\omega, \\ \boldsymbol{\Sigma}_2 &= \frac{1}{2\pi} \int_{-\infty}^{\infty} \mathbf{N}_{\mathcal{B}2}(i\omega) \mathbf{N}_{\mathcal{B}2}(i\omega)^* d\omega, \\ 0 &= \frac{1}{2\pi} \int_{-\infty}^{\infty} \mathbf{N}_{\mathcal{B}1}(i\omega) \mathbf{N}_{\mathcal{B}2}(i\omega)^* d\omega. \end{aligned}$$

Considering the first row of  $\mathbf{B}_{\mathcal{B}} = \mathbf{K}_{\mathcal{B}}(\cdot) \mathbf{N}_{\mathcal{B}}(\cdot)$ , we get  $\mathbf{B}_r = \mathbf{K}_r(\cdot) \mathbf{N}_{\mathcal{B}1}(\cdot) + \mathbf{K}_{12}(\cdot) \mathbf{N}_{\mathcal{B}2}(\cdot)$ . Define the reduced order quantity  $\mathbf{N}_r(\cdot) = \mathbf{K}_r(\cdot)^{-1} \mathbf{B}_r$ . Then, by substituting the expression for  $\mathbf{B}_r$  into this definition, we obtain

$$\mathbf{N}_r(\cdot) = \mathbf{N}_{\mathcal{B}1}(\cdot) + \mathbf{L}(\cdot) \mathbf{N}_{\mathcal{B}2}(\cdot),$$

with  $\mathbf{L}(\cdot) = \mathbf{K}_r(\cdot)^{-1} \mathbf{K}_{12}(\cdot)$ . Consider now the error norm

$$\begin{aligned} \|\mathfrak{H}_{\mathbf{G}} - \mathfrak{H}_{\mathbf{G}_r}\|_{\mathcal{H}_2}^2 &= \|\mathfrak{H}_{\mathbf{G}} - \mathfrak{H}_{\mathbf{G}_r}\|_{\mathcal{H}_2}^2 \\ &= \|\mathfrak{H}_{\mathbf{G}}\|_{\mathcal{H}_2}^2 - 2\text{Re}\{\langle \mathfrak{H}_{\mathbf{G}}, \mathfrak{H}_{\mathbf{G}_r} \rangle_{\mathcal{H}_2}\} + \|\mathfrak{H}_{\mathbf{G}_r}\|_{\mathcal{H}_2}^2, \end{aligned} \quad (34)$$

with the three developed terms being

$$\|\mathfrak{H}_{\mathbf{G}}\|_{\mathcal{H}_2}^2 = \text{trace}\{\mathbf{C}_r \boldsymbol{\Sigma}_1 \mathbf{C}_r^*\} + \text{trace}\{\mathbf{C}_2 \boldsymbol{\Sigma}_2 \mathbf{C}_2^*\}, \quad (35)$$

$$\begin{aligned} \langle \mathfrak{H}_{\mathbf{G}}, \mathfrak{H}_{\mathbf{G}_r} \rangle_{\mathcal{H}_2} &= \text{trace}\{\mathbf{C}_r \boldsymbol{\Sigma}_1 \mathbf{C}_r^*\} \\ &+ \frac{1}{2\pi} \int_{-\infty}^{\infty} \text{trace}\{\mathbf{C}_{\mathcal{B}} \mathbf{N}_{\mathcal{B}}(i\omega) \mathbf{N}_{\mathcal{B}2}(i\omega)^* \mathbf{L}(i\omega)^* \mathbf{C}_r^*\} d\omega, \end{aligned} \quad (36)$$

$$\begin{aligned} \|\mathfrak{H}_{\mathbf{G}_r}\|_{\mathcal{H}_2}^2 &= \text{trace}\{\mathbf{C}_r \boldsymbol{\Sigma}_1 \mathbf{C}_r^*\} \\ &+ 2\text{Re}\left\{\frac{1}{2\pi} \int_{-\infty}^{\infty} \text{trace}\{\mathbf{C}_r \mathbf{N}_{\mathcal{B}1}(i\omega) \mathbf{N}_{\mathcal{B}2}(i\omega)^* \mathbf{L}(i\omega)^* \mathbf{C}_r^*\} d\omega\right\} \\ &+ \frac{1}{2\pi} \int_{-\infty}^{\infty} \text{trace}\{\mathbf{C}_r \mathbf{L}(i\omega) \mathbf{N}_{\mathcal{B}2}(i\omega) \mathbf{N}_{\mathcal{B}2}(i\omega)^* \mathbf{L}(i\omega)^* \mathbf{C}_r^*\} d\omega. \end{aligned} \quad (37)$$

By plugging (35), (36), and (37) into (34) we get

$$\begin{aligned} \|\mathfrak{H}_{\mathbf{G}} - \mathfrak{H}_{\mathbf{G}_r}\|_{\mathcal{H}_2}^2 &= \text{trace}\{\mathbf{C}_2 \boldsymbol{\Sigma}_2 \mathbf{C}_2^*\} \\ &+ \text{Re}\left\{\frac{1}{2\pi} \int_{-\infty}^{\infty} \text{trace}\{(\mathbf{C}_r \mathbf{L}(i\omega) - 2\mathbf{C}_2) \right. \\ &\quad \left. \mathbf{N}_{\mathcal{B}2}(i\omega) \mathbf{N}_{\mathcal{B}2}(i\omega)^* \mathbf{L}(i\omega)^* \mathbf{C}_r^*\} d\omega\right\} \end{aligned}$$

with the bound

$$\begin{aligned} \|\mathfrak{H}_{\mathbf{G}} - \mathfrak{H}_{\mathbf{G}_r}\|_{\mathcal{H}_2}^2 &\leq \text{trace}\{\mathbf{C}_2 \boldsymbol{\Sigma}_2 \mathbf{C}_2^*\} \\ &+ \sup_{\omega} \|\mathbf{L}(i\omega)^* \mathbf{C}_r^* (\mathbf{C}_r \mathbf{L}(i\omega) - 2\mathbf{C}_2)\|_2 \text{trace}\{\boldsymbol{\Sigma}_2\}. \end{aligned} \quad \square$$

## 5 Numerical experiments

In this section, we test conformalBT on three numerical examples. While the spectrum of the full order system is in  $\mathbb{C}_-$  for the first example, it is in  $i\mathbb{R}_+$  for the second, and in  $i\mathbb{R}$  for the third. All the numerical experiments were generated on a Lenovo ThinkPad with an 8 core Intel<sup>®</sup> i7-8565U 1.8GHz processor, 48GB of RAM, and MATLAB R2023b. For all PDE examples, we used a spatial semi-discretization by centered finite differences.

To compute the conformal Gramians while the `lyapchol` command was used for the first two examples, in Section 5.1 and Section 5.2, an adaptive Gauss-Kronrod algorithm was used for the third example in Section 5.3 and its implementation follows the steps described in [7]. For the computation of the  $\mathcal{H}_2$  norms and the output trajectories we relied on the commands `integral` and `ode23`, respectively. Both the `ode23` and the `integral` functions adopt relative and absolute tolerances of  $10^{-8}$  and  $10^{-12}$ , respectively. The code to generate the numerical results is available at <https://github.com/aaborghi/conformalBT.git>

## 5.1 Heat equation

In the first example we consider the boundary controlled heat equation described as

$$\begin{aligned} \frac{\partial w(x, t)}{\partial t} &= \frac{\partial^2 w(x, t)}{\partial x^2}, & \text{on } (0, 1) \times (0, T), \\ w(0, t) &= 0, \quad w(1, t) = u(t), & \text{on } (0, T), \\ y(t) &= \int_{0.1}^{0.4} w(x, t) dx, & \text{on } (0, T), \\ w(x, 0) &= 0, & \text{in } (0, 1), \end{aligned}$$

where  $u$  and  $y$  are, respectively, the scalar input and output. The discretization results in a full order system of dimension  $n = 200$ ,  $q = m = 1$ , and poles in the negative real axis  $\mathbb{R}_-$ . This example was specifically chosen due to its spectrum being in the left-half plane so that we can compare the performance of `conformalBT` with that of classical balanced truncation. For the former we choose a Möbius transformation (5) that maps the left-half plane  $\mathbb{C}_-$  into the disk  $\mathbb{A} = \mathbb{D}_{R,c} = \{z \in \mathbb{C} \mid |z - c| < R\}$  and  $i\mathbb{R}$  to  $\partial\mathbb{D}_{R,c}$ . To do so, we choose the parameters  $\alpha, \beta, \gamma, \delta$  such that we have

$$\psi(\cdot) = c + R \frac{\cdot + 1}{\cdot - 1}. \quad (38)$$

Because  $\psi: \mathbb{C}_- \rightarrow \mathbb{D}_{R,c}$  is a mapping that satisfies the assumptions of [Theorem 3](#) we then have that `conformalBT` computes a ROM with poles in  $\mathbb{D}_{R,c}$ . As a matter of fact, plugging in the values of  $\alpha, \beta, \gamma$  and  $\delta$  of (38) in the inequality (28) results in

$$|\lambda - c|^2 < R^2,$$

which indicates the disk  $\mathbb{D}_{R,c}$ . A similar result can be found in [14, Example 3.4.104] by replacing  $\alpha, \beta, \gamma, \delta$  in (25) with  $R + c, R - c, 1, -1$ , respectively. To enclose the spectrum of the system we choose  $c = -17 \times 10^4$  and  $R = 17 \times 10^4$ . Recalling [Remark 2](#) we need the range of (38) to be a subset of  $\mathbb{C}_-$  so to avoid the potential placement of the ROM poles in the right half plane. For this reason we chose  $R = -c$ . Since (38) satisfies the assumptions in [Theorem 2](#), we compute the Gramians by solving the Lyapunov equations (19) and (20).

We present the  $\mathcal{H}_2(\bar{\mathbb{A}}^c)$  error norm along with the error bound in the top plot of [Fig. 2](#) for various  $r$  values. In addition, the bottom plot shows the output relative error of the impulse response for a reduced model with  $r = 10$  computed by `conformalBT` and BT. The result shows that the two algorithms reach the same level of accuracy.

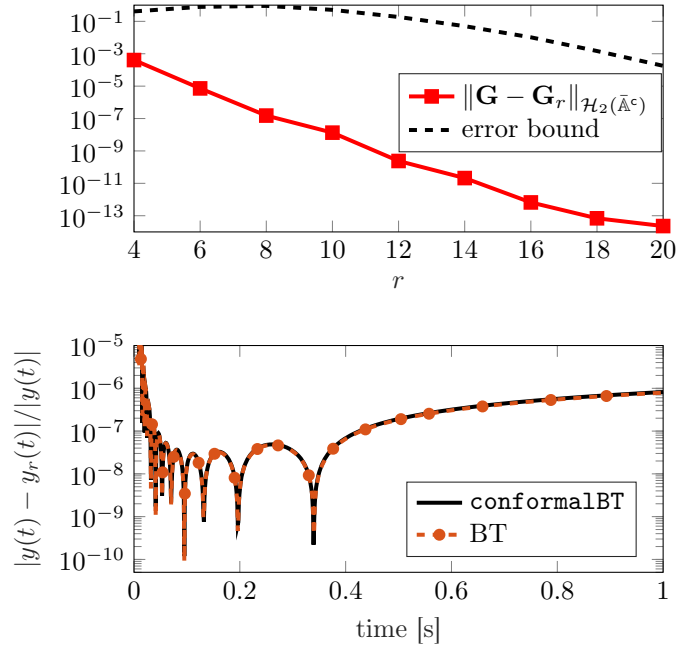


Figure 2: (Top)  $\mathcal{H}_2(\bar{\mathbb{A}}^c)$  error norm between the full and reduced order systems along with the  $\mathcal{H}_2$  error bound in (31) for different values of  $r$ . (Bottom) relative error of the ROM impulse response with  $r = 10$  computed with `conformalBT` and BT applied to the Heat equation with  $n = 200$ .

## 5.2 Schrödinger equation

In this example we test `conformalBT` as given in [Algorithm 1](#) on a controlled variant of the Schrödinger equation

$$\begin{aligned} \frac{\partial w(x, t)}{\partial t} &= -i \frac{\partial^2 w(x, t)}{\partial x^2} + \chi_{[0.4, 0.5]} u^{(1)}(t) \\ &\quad + \chi_{[0.5, 0.6]} u^{(2)}(t), & \text{on } (0, 1) \times (0, T), \\ w(0, t) &= 0, \quad w(1, t) = 0, & \text{on } (0, T), \\ \mathbf{y}(t) &= \begin{bmatrix} \int_{0.1}^{0.3} w(x, t) dx \\ \int_{0.7}^{0.9} w(x, t) dx \end{bmatrix}, & \text{on } (0, T), \\ w(x, 0) &= 0, & \text{in } (0, 1), \end{aligned}$$

where  $u^{(1)}$  and  $u^{(2)}$ , and  $\mathbf{y}$  are the inputs and outputs, respectively. After discretization, the differential equation results in a FOM with  $q = 2$ ,  $m = 2$ , and  $n = 1000$ . Because the spectrum of the system is on the upper part of the imaginary axis we choose the clockwise rotatory conformal map

$$\psi(\cdot) = -i \cdot \quad (39)$$

with  $\psi: \mathbb{C}_- \rightarrow \mathbb{C}_\uparrow$ , and  $\psi: i\mathbb{R} \rightarrow \mathbb{R}$ , where  $\mathbb{A} = \mathbb{C}_\uparrow$  is the open upper half complex plane. Similarly to [Section 5.1](#),

also here the conformal map chosen in (39) satisfies the assumptions in Theorem 3. As a matter of fact, plugging in the coefficients of the Möbius transformation in (39) into (28) results in the inequality  $\text{Im}(\lambda) > 0$ , which exactly defines  $\mathbb{C}_\uparrow$ . In addition, (39) satisfies also the assumptions in Theorem 2, allowing us to compute the Gramians by solving (19) and (20).

In the top plot of Fig. 3 we show the evolution of the  $\mathcal{H}_2(\bar{\mathbb{A}}^c)$  error norm between the FOM and the ROM computed with `conformalBT` for different reduced orders  $r$  along with the error bound given in Theorem 4. The middle plot shows the output relative error of the step response with  $r = 9$ . The spikes in the error are due to all the output signals reaching 0. It can be seen from the error plot that the resulting ROM output well approximates the FOM response given the control inputs  $u^{(1)} = u^{(2)} = \mathbf{u}$  showed in the bottom plot.

We note that since  $\psi$  satisfies the assumptions of Theorem 3, it is assured that the reduced system poles are in  $\mathbb{A} = \mathbb{C}_\uparrow$ , thus the reduced system retains stability in the sense of Theorem 3. However, this does not mean that the reduced poles will also exactly lie on the upper part of the imaginary axis since the upper half plane includes the upper-right and upper-left quadrants. This can result in a ROM that does not mirror the output behaviour of the full order system. In the next example we choose a conformal map designed to overcome this issue.

### 5.3 Undamped linear wave equation

The last example consists of the controlled wave equation

$$\begin{aligned} \frac{\partial^2 w(x, t)}{\partial t^2} &= \frac{\partial^2 w(x, t)}{\partial x^2} + \chi_{[0.1, 0.2]} u^{(1)}(t) \\ &\quad + \chi_{[0.8, 0.9]} u^{(2)}(t), && \text{on } (0, 1) \times (0, T), \\ w(0, t) &= 0, \quad w(1, t) = 0, && \text{on } (0, T), \\ \mathbf{y}(t) &= \begin{bmatrix} \int_{0.3}^{0.5} w(x, t) dx \\ \int_{0.6}^{0.7} w(x, t) dx \end{bmatrix}, && \text{on } (0, T), \\ w(x, 0) &= 0, && \text{in } (0, 1). \end{aligned}$$

After discretization we get a full order model with  $n = 5000$ ,  $q = 2$ , and  $m = 2$ . The spectrum of this system lies on the imaginary axis. We designed a function  $\psi$  based on the Joukowski transform that maps part of the left-half plane, including the imaginary axis, into a Bernstein ellipse  $\mathbb{B}$  excluding the strip  $[-1, 1]$ , i.e.,  $\mathbb{B} \setminus [-1, 1]$ . This is then translated by  $c \in \mathbb{C}$  and scaled by  $M \in \mathbb{C}$ . We refer to the resulting domain with and without the strip as  $\mathbb{B}_{M,c}$  and  $\mathbb{A} = \tilde{\mathbb{B}}_{M,c}$ , respectively. A thorough analysis of this function is given in [6, Section 4.1.3]. The corresponding

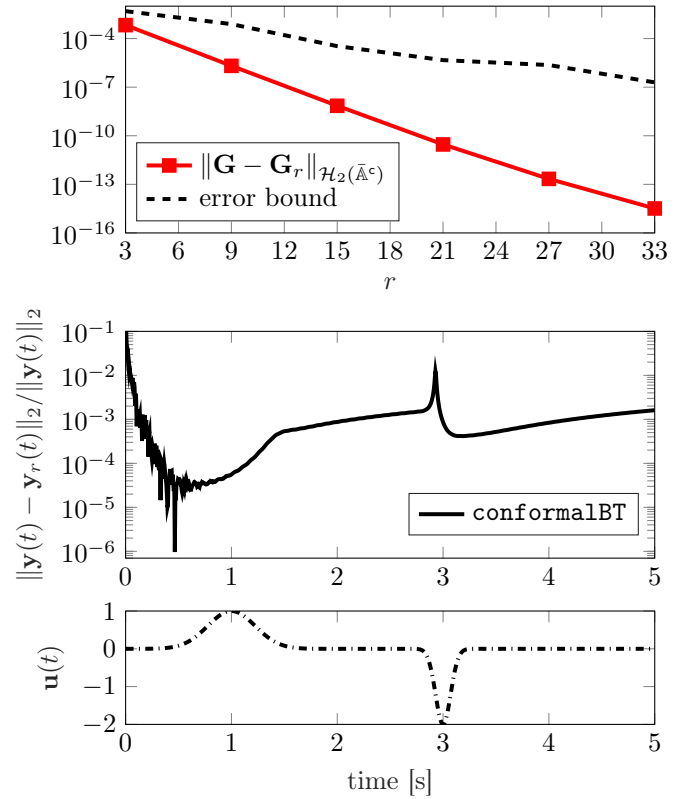


Figure 3: (Top)  $\mathcal{H}_2(\bar{\mathbb{A}}^c)$  error norm between the full and reduced order systems along with the  $\mathcal{H}_2$  error bound in (31) for different values of  $r$ . (Middle) relative error of the ROM step response with  $r = 9$  computed with `conformalBT` applied to the Schrödinger equation with  $n = 1000$ . (Bottom) Input adopted for evaluating `conformalBT`. Here,  $u^{(1)}$  and  $u^{(2)}$  follow the same trajectory equal to  $\mathbf{u}$ .

conformal map is defined as

$$\psi(\cdot) = c + \frac{M}{2} \left( R \frac{\cdot + 1}{\cdot - 1} + \frac{1 \cdot - 1}{R \cdot + 1} \right) \quad (40)$$

with  $\psi: \mathbb{X} \rightarrow \tilde{\mathbb{B}}_{M,c}$  and  $\psi: i\mathbb{R} \rightarrow \partial\mathbb{B}_{M,c}$ . Here,  $\mathbb{X}$  is a subset of  $\mathbb{C}_-$  that includes the imaginary axis and  $\partial\mathbb{B}_{M,c}$  coincides with  $\partial\mathbb{A}^+$  in Assumption 1.3. A graphical representation of (40) is showed in Fig. 4. To avoid computing reduced systems with poles off the imaginary axis, as discussed in Section 5.2, we choose the parameters of (40) such that the ellipse  $\partial\mathbb{B}_{M,c}$  has the minor semi-axis that is small enough for the set  $\tilde{\mathbb{B}}_{M,c}$  to cover the section of the imaginary axis with the FOM poles as closely as possible. Since (40) does not satisfy the assumptions of Theorem 2, we compute the Gramians by approximating (14) and (15) using the adap-

tive Gauss-Kronrod quadrature (see [7, Section 5.1] and citations therein). It is interesting to point out that, even if not proven, in this numerical example the poles of  $\mathbf{G}_r$  computed with Algorithm 1 lie inside  $\tilde{\mathbb{B}}_{M,c}$ . By keeping the minor semi-axis as small as possible we are able to keep the reduced model poles approximately on the imaginary axis. This is done by setting the value of  $R$  close to 1. Accordingly, we choose the following parameters for (40):  $R = 1 + 10^{-5}$ ,  $M = 10^4$ ,  $c = 10^{-6}$ . The disadvantage of decreasing the minor semi-axis is that the ellipse contour approaches the spectrum of the full order model. This makes the offline computation of the Gramians computationally expensive as the adaptive Gauss-Kronrod needs to refine the integration interval several times. Nevertheless, the resulting ROM computed by conformalBT with  $r = 40$  have its poles almost nearly on the imaginary axis with a maximum real part of approximately  $\pm 10^{-10}$ , thus fulfilling our objective. Fig. 5 shows the impulse response of the discretized wave equation compared to the reduced model computed by conformalBT. The error in the bottom plot of Fig. 5 shows that the resulting ROM output provides a high-fidelity approximation to the FOM output dynamics.

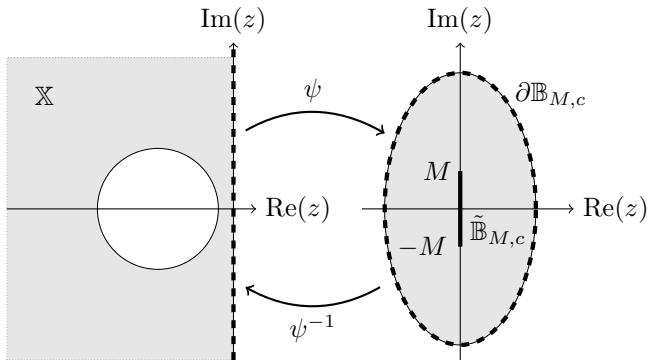


Figure 4: A depiction of the conformal map in (40) centered at the origin ( $c = 0$ ). The grey sets on the left and on the right are, respectively, the domain and range of  $\psi$ . Here we have the scaling being  $M \in \mathbb{i}\mathbb{R}$ . The thick line in  $\tilde{\mathbb{B}}_{M,c}$  indicates the strip  $[-1, 1]$  after the scaling.

## 6 Conclusions

In this paper, we presented a new balanced truncation framework which allows the treatment of transfer functions with poles in general domains. We adopted conformal maps and the  $\mathcal{H}_2(\mathbb{A}^c)$  space to define the Gramians related to these particular systems. We showed that when the Möbius transformation is used as conformal map, it is possible to com-

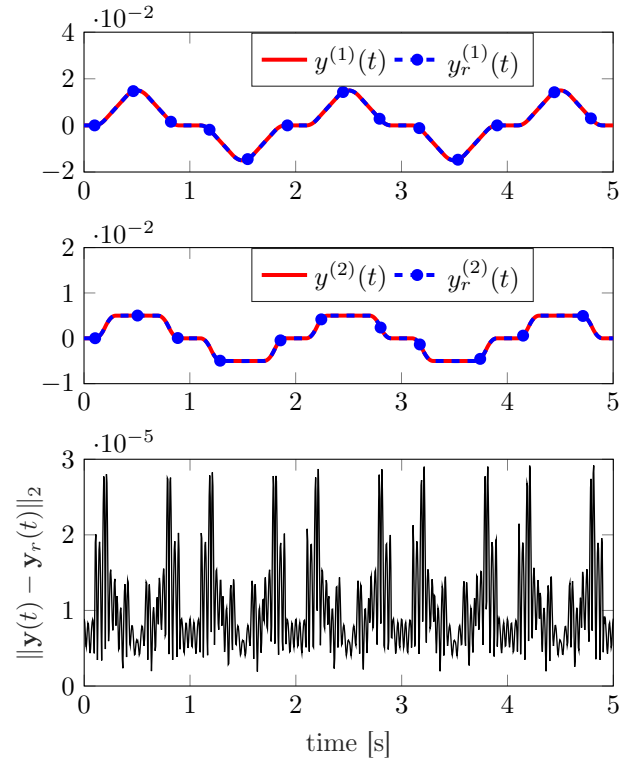


Figure 5: (Top) impulse response of the full and reduced order systems,  $y^{(i)}$  and  $y_r^{(i)}$ , respectively, with  $i = 1, 2$ . Here conformalBT computed an  $r = 40$  reduced order model on a discretized wave equation with  $n = 5000$ . (Bottom) the output error.

pute the new Gramians by solving modified Lyapunov equations. For the proposed algorithm conformalBT we proved that the resulting reduced model has a bounded  $\mathcal{H}_2$  error norm and that, when the Möbius transformation is adopted, it preserves the stability of the original full order system.

## Acknowledgments

We would like to thank Jesper Schröder for his helpful discussions. The work of Borghi and Breiten was funded by the Deutsche Forschungsgemeinschaft (DFG, German Research Foundation) - 384950143 as part of GRK2433 DAEDALUS. Gugercin's work was supported in part by the US National Science Foundation under Grant CMMI-2130727.

## Conflict of interest

The authors declare no competing interests.

## References

- [1] Antoulas, A.C.: Approximation of Large-Scale Dynamical Systems. Society for Industrial and Applied Mathematics (2005). doi:[10.1137/1.9780898718713](https://doi.org/10.1137/1.9780898718713)
- [2] Antoulas, A.C., Beattie, C.A., Gugercin, S.: Interpolatory Methods for Model Reduction. Society for Industrial and Applied Mathematics, Philadelphia, PA (2020). doi:[10.1137/1.9781611976083](https://doi.org/10.1137/1.9781611976083)
- [3] Benner, P., Grivet-Talocia, S., Quarteroni, A., Rozza, G., Schilders, W., Silveira, L. (eds.): Volume 1 System- and Data-Driven Methods and Algorithms. De Gruyter, Berlin, Boston (2021). doi:[10.1515/9783110498967](https://doi.org/10.1515/9783110498967)
- [4] Benner, P., Mehrmann, V., Sorensen, D.: Dimension Reduction of Large-Scale Systems. Springer, Berlin, Germany (2005). doi:[10.1007/3-540-27909-1](https://doi.org/10.1007/3-540-27909-1)
- [5] Benner, P., Ohlberger, M., Cohen, A., Willcox, K.: Model reduction and approximation: theory and algorithms. Society for Industrial and Applied Mathematics, Philadelphia, PA (2017). doi:[10.1137/1.9781611974829](https://doi.org/10.1137/1.9781611974829)
- [6] Borghi, A., Breiten, T.:  $\mathcal{H}_2$  optimal rational approximation on general domains. *Advances in Computational Mathematics* **50**, 28 (2024). doi:[10.1007/s10444-024-10125-8](https://doi.org/10.1007/s10444-024-10125-8)
- [7] Breiten, T.: Structure-preserving model reduction for integro-differential equations. *SIAM Journal on Control and Optimization* **54**(6), 2992–3015 (2016). doi:[10.1137/15M1032296](https://doi.org/10.1137/15M1032296)
- [8] Breiten, T., Stykel, T.: Balancing-related model reduction methods. In: P. Benner, S. Grivet-Talocia, A. Quarteroni, G. Rozza, W. Schilders, L.M. Silveira (eds.) *Model Order Reduction*, vol. 1 System- and Data-Driven Methods and Algorithms. De Gruyter, Berlin, Boston (2021). doi:[10.1515/9783110498967-002](https://doi.org/10.1515/9783110498967-002)
- [9] Davies, P.I., Higham, N.J.: A Schur-Parlett algorithm for computing matrix functions. *SIAM Journal on Matrix Analysis and Applications* **25**(2), 464–485 (2003). doi:[10.1137/S0895479802410815](https://doi.org/10.1137/S0895479802410815)
- [10] Duren, P.: *Theory of  $H^p$  Spaces*. Academic Press, New York and London (1970). doi:[10.1016/S0079-8169\(08\)62674-4](https://doi.org/10.1016/S0079-8169(08)62674-4)
- [11] Gosea, I.V., Gugercin, S., Beattie, C.: Data-driven balancing of linear dynamical systems. *SIAM Journal on Scientific Computing* **44**(1), A554–A582 (2022). doi:[10.1137/21M1411081](https://doi.org/10.1137/21M1411081)
- [12] Gugercin, S., Antoulas, A.C.: A survey of model reduction by balanced truncation and some new results. *International Journal of Control* **77**(8), 748–766 (2004). doi:[10.1080/00207170410001713448](https://doi.org/10.1080/00207170410001713448)
- [13] Higham, N.J.: *Functions of Matrices*. Society for Industrial and Applied Mathematics (2008). doi:[10.1137/1.9780898717778](https://doi.org/10.1137/1.9780898717778)
- [14] Hinrichsen, D., Pritchard, A.J.: *Mathematical Systems Theory I*. Springer Berlin, Heidelberg (2005). doi:[10.1007/b137541](https://doi.org/10.1007/b137541)
- [15] Moore, B.: Principal component analysis in linear systems: Controllability, observability, and model reduction. *IEEE Transactions on Automatic Control* **26**(1), 17–32 (1981). doi:[10.1109/TAC.1981.1102568](https://doi.org/10.1109/TAC.1981.1102568)
- [16] Mullis, C., Roberts, R.: Synthesis of minimum round-off noise fixed point digital filters. *IEEE Transactions on Circuits and Systems* **23**(9), 551–562 (1976). doi:[10.1109/TCS.1976.1084254](https://doi.org/10.1109/TCS.1976.1084254)
- [17] Quarteroni, A., Manzoni, A., Negri, F.: Reduced basis methods for partial differential equations: an introduction. UNITEXT. Springer Cham (2016). doi:[10.1007/978-3-319-15431-2](https://doi.org/10.1007/978-3-319-15431-2)
- [18] Sorensen, D., Antoulas, A.C.: Dimension Reduction of Large-Scale Systems, chap. On Model Reduction of Structured Systems, p. 117–130. Springer Berlin Heidelberg (2005). doi:[10.1007/3-540-27909-1\\_4](https://doi.org/10.1007/3-540-27909-1_4)
- [19] Volkwein, S.: Proper orthogonal decomposition: Theory and reduced-order modelling. *Lecture Notes*, Department of Mathematics and Statistics University of Konstanz, University of Graz (2013)
- [20] Wegert, E.: *Visual Complex Functions*. Springer, Basel, Switzerland (2012). doi:[10.1007/978-3-0348-0180-5](https://doi.org/10.1007/978-3-0348-0180-5)